

grown axenically *in vitro* using supplemented RPMI 1640 medium, and at intervals after the stationary phase (21 days) they were passaged into new cultures containing each drug or both drugs (hygromycin, 150 µg ml<sup>-1</sup>; G418, 120 µg ml<sup>-1</sup>). Second, mammalian cell (Vero) monolayers were infected with P1-*hyg* and P2-*neo* using stationary-phase, mixed axenic cultures containing epimastigotes and metacyclic trypomastigotes. Trypomastigotes from pseudocysts were recovered periodically between days 7 and 28, and grown as epimastigotes in axenic culture for drug sensitivity tests. Third, triatomine bugs were membrane fed on mouse blood containing P1-*hyg* and P2-*neo* trypomastigotes derived from Vero cell monolayers. Bugs were dissected 25–30 days later, *T. cruzi* was re-isolated by culture on biphasic blood agar, and was passaged into axenic culture to obtain sufficient organisms for testing drug sensitivities. Last, groups of three immunocompromised (SCID) mice were inoculated with a mixture of faeces from triatomine bugs carrying P1-*hyg* or P2-*neo*. Populations were subsequently retrieved from infected mice into axenic culture and placed under drug pressure.

**Determination of phenotype and genotype**

DNA purification was carried out by phenol/chloroform extraction and ethanol precipitation or using DNeasy (Qiagen). Amplification reactions used the following conditions: denaturation for 5 min at 94 °C, then 30 cycles of 94 °C (1 min), 50–62 °C (1 min; depending on the primer *T<sub>m</sub>*) and 72 °C (1 min per 1,000 bp), followed by 10 min at 72 °C. Primers are described in Supplementary appendix 6. PGM phenotype determination and RAPD analysis were as described previously<sup>6</sup>. Episomes were detected by multiplex amplification using primers designed to the hygromycin phosphotransferase and neomycin phosphotransferase genes. For karyotype analysis we used a Bio-Rad CHEF Mapper with an autoalgorithm for separation of 0.4–2.2-Mb fragments, followed by Southern blotting and hybridization with radiolabelled probes.

The following DNA sequences were amplified, some with *Taq* Extender; Stratagene: (1) *tpm1*<sup>19</sup> (trypanoxin; GenBank accession number AF106855; 435 bp); (2) *gpi* (1,038 bp); (3) putative *pgm* (380 bp) (TIGR database (<http://www.tigr.org>) accession number TC1375), identified by similarity between human and putative *Leishmania* *pgm*; (4) *tcp*, an intergenic region (760 bp, including gaps) flanked by 3' *tcp17* and partial 5' *tcpgp2* (ref. 20); (5) a mitochondrial locus (1,078 bp) spanning the maxicircle-encoded genes cytochrome oxidase subunit II (*colII*) and *nd1* (ref. 3); and (6) *dhfr-ts* (1,042 bp)<sup>3</sup>. PCR products from all loci were cloned into pGEM T (Promega), except where no heterozygous alleles were detectable (mitochondrial DNA<sup>3</sup> of progeny; *gpi* of some isolates). For each isolate a minimum of three (*gpi*) and either three or six (*tcp*) clones were sequenced on a capillary sequencer (Beckman) or an ABI 377 using relevant kits.

Genotypes were also determined at eight microsatellite loci<sup>13</sup>, with primers labelled with FAM, NED and HEX, and sized against the ROX 500 marker (ABI) using an ABI 377. An additional 12 microsatellite loci were identified by searching the *T. cruzi* genome database for dinucleotide repeats (TIGR database; see also Supplementary appendix 7). GenScan and Genotyper software (Applied Biosystems) were used to automate measurements of allele length. All microsatellite loci were amplified from P1-*hyg* and P2-*neo* and their double-drug-resistant progeny using standard conditions; a subset (MCLE01, MCLEF10, MCLEG10, SCLE10 and SCLE11 (ref. 13), and A427, A831.3, E801, J356 and N060 (Supplementary appendix 7)) was amplified from all reference strains and field isolates (Supplementary appendix 8).

**Phylogenetic analysis**

Nucleotide sequences were aligned using Clustal X<sup>27</sup> then edited by hand, and are available on request. Primarily, sites of recombination were examined by bootscan analysis<sup>28</sup> using the Kimura two-parameter model. Recombination sites were investigated further by maximum likelihood breakpoint analysis<sup>29</sup>. All maximum likelihood parameter estimates comprising a four-category gamma distribution and a transition/transversion ratio ( $\kappa$ ) were obtained with the tree bisection reconnection (TBR) heuristic search (where reconnection limit = 4) using PAUP\* 4.0b (D. L. Swofford). Each data set of field isolates and reference strains was also subject to refined split decomposition analysis (Kimura three-parameter model)<sup>30</sup>.

Received 11 October 2002; accepted 14 January 2003; doi:10.1038/nature01438.

1. Cook, G. C. & Zumla, A. (eds) *Manson's Tropical Diseases* (Saunders, London, 2003).
2. World Health Organisation. *Control of Chagas Disease* (World Health Organisation Technical Report Series 905, Geneva, 2002).
3. Machado, C. A. & Ayala, F. J. Nucleotide sequences provide evidence of genetic exchange among distantly related lineages of *Trypanosoma cruzi*. *Proc. Natl Acad. Sci. USA* **98**, 7396–7401 (2001).
4. Gibson, W. C. & Stevens, J. R. Genetic exchange in the trypanosomatidae. *Adv. Parasitol.* **43**, 1–46 (1999).
5. Bingle, L. E., Eastlake, J. L., Bailey, M. & Gibson, W. C. A novel GFP approach for the analysis of genetic exchange in trypanosomes allowing the *in situ* detection of mating events. *Microbiology* **147**, 3231–3240 (2001).
6. Carrasco, H. J., Frame, I. A., Valente, S. A. & Miles, M. A. Genetic exchange as a possible source of genomic diversity in sylvatic populations of *Trypanosoma cruzi*. *Am. J. Trop. Med. Hyg.* **54**, 418–424 (1996).
7. Gibson, W. C. & Bailey, M. Genetic exchange in *Trypanosoma brucei*: evidence for meiosis from analysis of a cross between drug-resistant transformants. *Mol. Biochem. Parasitol.* **64**, 241–252 (1996).
8. Stothard, J. R., Frame, I. A. & Miles, M. A. Genetic diversity and genetic exchange in *Trypanosoma cruzi*: dual drug-resistant 'progeny' from episomal transformants. *Mem. Inst. Oswaldo Cruz* **94** Suppl. 1, 189–193 (1999).
9. Ohno, S. *Evolution by Gene Duplication* (Springer, Berlin, 1970).
10. Knight, J. All genomes great and small. *Nature* **417**, 374–376 (2002).
11. Brisse, S., Barnabe, C. & Tibayrenc, M. Identification of six *Trypanosoma cruzi* phylogenetic lineages by random amplified polymorphic DNA and multilocus enzyme electrophoresis. *Int. J. Parasitol.* **30**, 35–44 (2000).

12. Mendonca, M. B. *et al.* Two main clusters within *Trypanosoma cruzi* zymodeme 3 are defined by distinct regions of the ribosomal RNA cistron. *Parasitology* **124**, 177–184 (2002).
13. Oliveira, R. P. *et al.* Probing the genetic population structure of *Trypanosoma cruzi* with polymorphic microsatellites. *Proc. Natl Acad. Sci. USA* **95**, 3776–3780 (1998).
14. Miles, M. A. *et al.* Do radically dissimilar *Trypanosoma cruzi* strains (zymodemes) cause Venezuelan and Brazilian forms of Chagas disease? *Lancet* **1**, 1338–1340 (1981).
15. Gaunt, M. W. & Miles, M. A. The ecotopes and evolution of triatomine bugs (Triatominae) and their associated trypanosomes. *Mem. Inst. Oswaldo Cruz* **95**, 557–565 (2000).
16. Tibayrenc, M. & Ayala, F. J. The clonal theory of parasitic protozoa: 12 years on. *Trends Parasitol.* **18**, 405–410 (2002).
17. McDaniel, J. P. & Dvorak, J. A. Identification, isolation, and characterization of naturally-occurring *Trypanosoma cruzi* variants. *Mol. Biochem. Parasitol.* **57**, 213–222 (1993).
18. Kelly, J. M. Genetic transformation of parasitic protozoa. *Adv. Parasitol.* **39**, 227–270 (1997).
19. Wilkinson, S. R. *et al.* The *Trypanosoma cruzi* enzyme TcGPXI is a glycosomal peroxidase and can be linked to trypanothione reduction by glutathione or trypanredoxin. *J. Biol. Chem.* **277**, 17062–17071 (2002).
20. Robello, C., Gamarro, F., Castanys, S. & Alvarez-Valin, F. Evolutionary relationships in *Trypanosoma cruzi*: molecular phylogenetics supports the existence of a new major lineage of strains. *Gene* **246**, 331–338 (2000).
21. MacLeod, A. *et al.* Minisatellite marker analysis of *Trypanosoma brucei*: reconciliation of clonal, panmictic, and epidemic population genetic structures. *Proc. Natl Acad. Sci. USA* **97**, 13442–13447 (2000).
22. Spratt, B. G. & Maiden, M. C. J. Bacterial population genetics, evolution and epidemiology. *Phil. Trans. R. Soc. Lond. B* **354**, 701–710 (1999).
23. Channanpant, J., Shan, W. X. & Tyler, B. M. High frequency mitotic gene conversion in genetic hybrids of the oomycete *Phytophthora sojae*. *Proc. Natl Acad. Sci. USA* **98**, 14530–14535 (2001).
24. Cruz, A. K., Titus, R. & Beverley, S. M. Plasticity in chromosome number and testing of essential genes in *Leishmania* by targeting. *Proc. Natl Acad. Sci. USA* **90**, 1599–1603 (1993).
25. Gaunt, M. W. & Miles, M. A. A molecular clock for the insects dates the origin of the insects and accords with paleontological and biogeographic landmarks. *Mol. Biol. Evol.* **19**, 748–761 (2002).
26. Miles, M. A. in *Protocols in Molecular Parasitology* (ed. Hyde, J. E.) 15–28 (Humana, Totowa, New Jersey, 1992).
27. Thompson, J. D., Gibson, T. J., Plewniak, F., Jeanmougin, F. & Higgins, D. G. CLUSTAL\_X windows interface: flexible strategies for multiple sequence alignment aided by quality analysis tools. *Nucleic Acids Res.* **25**, 4876–4882 (1997).
28. Salminen, M. O., Carr, J. K., Burke, D. S. & McCutchan, F. E. Identification of breakpoints in intergenotypic recombinants of HIV type 1 by bootscanning. *AIDS Res. Hum. Retrov.* **11**, 1423–1425 (1995).
29. Holmes, E. C., Worobey, M. & Rambaut, A. Phylogenetic evidence for recombination in dengue virus. *Mol. Biol. Evol.* **16**, 405–409 (1999).
30. Dopazo, J., Dress, A. & Vonhaeseler, A. Split decomposition—a technique to analyse viral evolution. *Proc. Natl Acad. Sci. USA* **90**, 10320–10324 (1993).

**Supplementary Information** accompanies the paper on Nature's website (<http://www.nature.com>).

**Acknowledgements** We thank the Wellcome Trust for financial support, D. Conway for valuable advice, and S. Wilkinson, S. Obado and J. Kelly for gifts of primers and comments on the manuscript.

**Competing interests statement** The authors declare that they have no competing financial interests.

**Correspondence** and requests for materials should be addressed to M.A.M. (e-mail: michael.miles@lshtm.ac.uk).

**Water transport in plants obeys Murray's law**

**Katherine A. McCulloh, John S. Sperry & Frederick R. Adler**

*Department of Biology, University of Utah, Salt Lake City, Utah 84112, USA*

The optimal water transport system in plants should maximize hydraulic conductance (which is proportional to photosynthesis<sup>1–5</sup>) for a given investment in transport tissue. To investigate how this optimum may be achieved, we have performed computer simulations of the hydraulic conductance of a branched transport system. Here we show that the optimum network is not achieved by the commonly assumed pipe model of plant form<sup>6–8</sup>, or its antecedent, da Vinci's rule<sup>9,10</sup>. In these representations, the number and area of xylem conduits is constant at

every branch rank. Instead, the optimum network has a minimum number of wide conduits at the base that feed an increasing number of narrower conduits distally. This follows from the application of Murray's law, which predicts the optimal taper of blood vessels in the cardiovascular system<sup>11</sup>. Our measurements of plant xylem indicate that these conduits conform to the Murray's law optimum as long as they do not function additionally as supports for the plant body.

The idea that organisms may be optimally designed has fuelled considerable research and controversy<sup>12–15</sup>. Both animals and plants require extensive and expensive transport systems, for which an optimal design presumably provides a selective advantage. In plants, transport through xylem has allowed growth in height and colonization of diverse habitats<sup>16</sup>, and must be extensive because photosynthesis entails an exchange of large quantities of internal water for atmospheric carbon dioxide. Plants use capillary suction to transport water from the roots to the leaves without using metabolic energy, and the xylem conduits themselves are cheap to maintain, being dead at maturity. However, the numerous thick-walled conduits require considerable carbon investment. This cost, combined with the benefit to photosynthesis of optimizing xylem design, implies that it would be advantageous for plants to maximize hydraulic conductance per vascular investment, and hence, to obey Murray's law<sup>11</sup>.

In 1926, Murray<sup>11</sup> developed a theory of optimal cardiovascular design that solves for the sizes of blood vessels from the aorta through progressive branch points to the capillaries that maximize the hydraulic conductance of flow through the vascular network for a fixed investment in blood and vessel volume. Under ideal conditions, the optimal design equalizes the sum of all radii cubed ( $\Sigma r^3$ ) at all points along the flow path if the volume flow rate ( $Q$ ) of the blood is conserved within the vascular system and the flow is laminar<sup>11</sup>. This result, known as Murray's law, fits data better than equalizing the sum of radii raised to the second or fourth powers<sup>17–19</sup>. Surprisingly, this law has not been systematically applied and tested in plant vasculature<sup>20</sup>.

Murray's law is applicable to plant xylem given the following four conditions. (1) The steady-state xylem  $Q$  is constant along the flow path. With the exception of the absorbing roots and the minor leaf veins, there will be no net loss of water from the xylem to surrounding tissues under steady-state conditions. (2) Xylem hydraulic conductance is proportional to conduit radius raised to the fourth power. This is the Hagen–Poiseuille prediction for laminar flow through cylindrical capillaries, which are appropriate

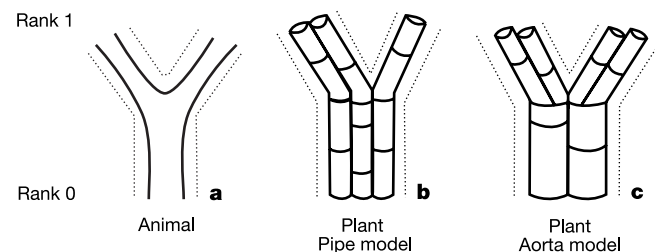


**Figure 1** Transport networks. **a**, Vascular networks in animals; **b, c**, plant xylem. The most proximal rank (rank 0) branches to form progressively distal ranks (for example, rank 1). In the animal cardiovascular system (**a**), a single continuous tube ramifies and the number of branches increases by an integer factor (the conduit furcation number,  $F$ ) between ranks. In the plant system, tubes are not continuous, but divided into conduits. Hundreds of conduits run in parallel within each branch (only a few are shown for clarity). In the 'pipe model' (**b**), the number of conduits is identical regardless of rank, and  $F = 1$ . In the 'aorta model' (**c**) the number of conduits increases with the number of branches by an integer factor as in the animal system, and  $F = 2$ . The pipe and aorta models are points in a continuum, because with hundreds of conduits in a single branch,  $F$  can be a fraction.

approximations for low-velocity xylem flow. (3) Conduit wall volume is proportional to total conduit volume. Murray assumed that the major volume cost was in the blood, and that the thin walls of blood vessels were negligible. In plants it is the opposite: the xylem water is cheap, but the conduit walls are costly. Murray's law is still valid, as long as the conduit wall volume scales directly with total conduit volume. The wall volume/conduit volume is proportional to the cavitation resistance of xylem<sup>21</sup>, as is necessary to withstand the compressive forces on the wall caused by negative pressure. Thus, for a given cavitation resistance throughout the xylem network, Murray's law should apply. (4) The xylem conduits must function primarily in transport, as opposed to providing an additional mechanical support role. When conduits are serving both functions (as in conifer shoots or diffuse-porous trees), the optimization criteria must include mechanical as well as hydraulic considerations, and Murray's law is inappropriate.

Murray's law by itself is not sufficient to characterize the conductance versus investment trade-off in xylem, because of fundamental structural differences between the vasculature of animals and plants. Figure 1a illustrates the single-branched tube of the animal network. As the single parent tube at rank 0 (for example, the

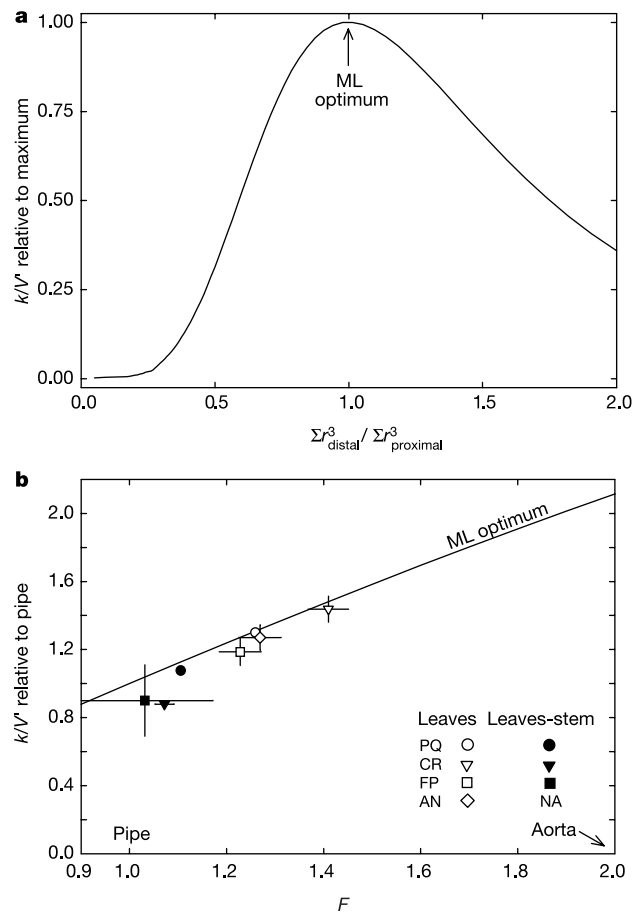


**Figure 2** Murray's law. **a**, The Murray's law (ML) optimum. The line shows relative hydraulic conductance ( $k$ ) per fixed volume ( $V^2$ ) plotted against the ratio of the sum of conduit radii cubed ( $\Sigma r^3$ ) of distal:proximal ranks in a modelled vascular network. The maximum  $k/V^2$  occurs at a  $\Sigma r^3$  ratio of 1 according to Murray's law regardless of the conduit furcation number ( $F$ ). **b**, The Murray law optimum versus  $F$ . The optimum is set to 1 for  $F = 1$  (pipe model). The greater efficiency of wide, proximal conduits in systems with higher  $F$  increases the hydraulic conductance for a given volume over the pipe model. The symbols show the measured  $F$  relative to the mean Murray's law optimum within leaves (open symbols,  $\pm$ s.d.) and comparing petioles with stems (filled symbols,  $\pm$ s.d.). PQ, *Parthenocissus quinquefolia* (vine); CR, *Campsis radicans* (vine); FP, *Fraxinus pennsylvanica* (ring-porous tree); and AN, *Acer negundo* (diffuse-porous tree).

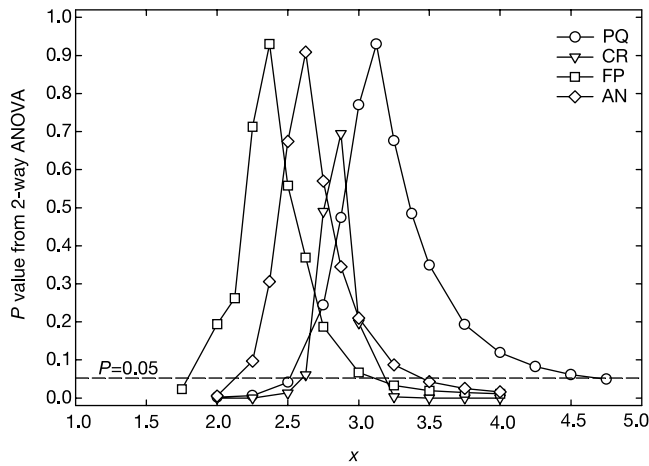


**Figure 3** ANOVA *P* values comparing the sum of the conduit radii raised to the *x* power ( $\Sigma r^x$ ) between petiolule versus petiole ranks of compound leaves. The *P* values are shown versus the exponent *x*. As the *P* value approaches 1, differences in  $\Sigma r^x$  between ranks are minimized. Although Murray's law predicts the maximum *P* value at *x* = 3, the law cannot be rejected if *P* at *x* = 3 is above 0.05 (dashed line). None of the *P* values at *x* = 3 were below 0.05.

aorta) branches into daughter tubes at rank 1, the number of tubes increases by a predictable integer factor, here referred to as the conduit furcation number (*F*). Such a system would be disastrous in plants because the xylem sap is under negative pressure, and a single injury would fill the entire network with air. Instead, the main stem of a plant at rank 0 has numerous conduits arranged in parallel and series, which can confine any dysfunction to a single conduit. Unlike the animal system, there is no constraint on *F*. For example, in Fig. 1b, the number of conduits stays the same across ranks; this configuration has become known as the ‘pipe model’<sup>6,22</sup> (*F* = 1). Alternatively, the conduits can increase with branch rank by the same integer factor as in the animal system (Fig. 1c, ‘aorta model’), but with multiple ‘aortas’ at rank 0 (*F* = 2). The pipe versus aorta distinctions are points in a continuum because *F* need not be an integer.

How does the pipe versus aorta configuration influence the trade-off between vascular conductance and investment? Regardless of *F*, the modelled maximum hydraulic conductance per vascular volume always occurs when  $\Sigma r^3$  is conserved throughout the system (Fig. 2a). This can also be shown by incorporating *F* in the derivation of Murray's law (Supplementary Information). However, the absolute value of the optimum increases with *F* (Fig. 2b). The pipe model yields substantially lower hydraulic conductance than the aorta model. The aorta model achieves greater conductance per volume by exploiting the increased efficiency of fewer, wider conduits in the proximal ranks.

The data in Fig. 2 raise the question of where real plants fall with respect to optimal conductance per volume. We put forward the hypothesis that xylem networks that meet the four assumptions of Murray's law should fall on the optimum with an *F* > 1 to exploit

the efficiency of fewer, wider conduits proximally. This hypothesis was tested in three contexts where the xylem conduit network does not perform a major mechanical support function: compound leaves, vines, and ring-porous trees (Table 1). Leaves are supported by turgor pressure and collenchyma, not xylem conduits. Compound leaves were chosen because there is no change in *Q* between petiolule and petiole ranks, unlike between ranks within leaf blade venation where *Q* is lost to transpiration. Vines are structural parasites, being supported by other plants or structures. In ring-porous trees, fibres provide the bulk of the structural support and the vessels comprise a relatively small fraction of the wood<sup>21</sup>.

The data for compound leaves were consistent with Murray's law. Figure 3 shows the results of the petiolule versus petiole comparison in four species (Table 1). The  $\Sigma r^x$  comparisons across ranks yielded maximum values of *P* for *x* between 2.4 and 3.2. In no species was the *P* value for *x* = 3 less than 0.05 (Fig. 3, dashed line), meaning that the  $\Sigma r^3$  was not significantly different between ranks. The shoot xylem of vine and ring-porous tree species was also generally consistent with Murray's law. Two out of the three petiolule versus stem comparisons had a *P* value for *x* = 3 greater than 0.05. The one deviant was only slightly different with the closest *x* at *P* > 0.05 equal to 2.85 (data not shown).

The proximity of each comparison to the Murray optimum is shown by the symbols in Fig. 2b. All comparisons had *F* > 1 as predicted, and there was a significant trend for xylem closest to Murray's law to have the greatest *F* value (Kendall's coefficient of rank correlation, *P* < 0.05 (ref. 23), symbols in Fig. 2b). The greatest *F* of 1.45 fell short of the aorta model (*F* = 2), perhaps because the increase in efficiency is offset by the reduction of conduit number in proximal stems and their increasing diameter (Table 1)—both factors can render the system vulnerable to failure<sup>24</sup>. Importantly, the situations in which *F* was greatest always occurred in the leaves, which are constructed specifically as disposable organs. Leaf versus stem comparisons tended to have greater  $\Sigma r^3$  in proximal versus distal ranks, and lower *F* (Fig. 2b, filled symbols).

Despite considerable interest in the adaptive significance of plant form, we are still far from understanding it. Quantifying the applicability of Murray's law is just one piece of the puzzle. Nevertheless, it improves upon Leonardo da Vinci's ‘rule’ that the total cross-sectional area of a tree's stems must be constant across branch ranks (area-preserving branching) to adequately supply the leaves<sup>9,10</sup>. The Murray optimum at *F* > 1 requires an increase in conduit cross-sectional area along the branched flow path (Table 1). The interaction between hydraulic supply and mechanical support of plant canopies undoubtedly underlies the distribution of supply versus support tissue in shoot structure. The two requirements are in conflict, because the optimal distribution of a fixed volume of tissue to support the tallest column requires a reduction in tissue area with height<sup>25,26</sup>.

The allometry of plant form predicts large-scale biological consequences—from the scaling between physiological processes and body size to the energy budgets of ecosystems. Recent work shows how a very specific plant vascular organization (the pipe model with *F* = 1) and branching pattern (exact self-similarity with no apical dominance) that functions at the equivalent of the Murray's law

**Table 1** Conduit number, mean radii and area

Rank	PQ (vine, <i>n</i> = 3)			CR (vine, <i>n</i> = 3)			FP (ring-porous, <i>n</i> = 3)			AN (diffuse-porous, <i>n</i> = 4)		
	CN	<i>r</i> (μm)	CA	CN	<i>r</i> (μm)	CA	CN	<i>r</i> (μm)	CA	CN	<i>r</i> (μm)	CA
Petiolule	10.4 (0.4)	17.08 (0.3)	2.6 (0.1)	17.7 (3.0)	13 (1.0)	2.5 (0.7)	3.0 (1.2)	19.9 (1.2)	1.1 (0.3)	1.8 (0.1)	18.4 (0.9)	1.2 (0.1)
Petiole	5.2 (0.1)	21.7 (0.6)	2.1 (0.2)	3.5 (0.6)	21.7 (1.8)	1.4 (0.3)	1.5 (0.6)	26.7 (2.1)	1 (0.3)	1 (0)	23.8 (2.3)	1 (0)
1-yr bud scar	1 (0)	35.8 (1.9)	1 (0)	1 (0)	32.6 (5.6)	1 (0)	1 (0)	24 (5)	1 (0)	NA	NA	NA

Branch ranks, relative change in total conduit number versus most proximal rank (CN), average conduit radius (*r*), and relative change in total conduit area versus most proximal rank (CA) for each species. The standard deviation from the mean of the individuals is listed in parentheses. PQ, *Parthenocissus quinquefolia* (vine); CR, *Campsis radicans* (vine); FP, *Fraxinus pensylvanica* (ring-porous tree); AN, *Acer negundo* (diffuse-porous tree). *n*, number of individuals measured per species. NA, not applicable. The 1-yr-old wood of *A. negundo* was not measured because the wood area is largely composed of conduits, which should contribute to the structural support of the plant.

optimum can be extrapolated to explain metabolic scaling rules in biology<sup>6–8</sup>. The challenge is to relax the unrealistic structural assumptions of these models and evaluate hydraulic and mechanical optima. We have seen that  $F$  is not necessarily 1, and we have determined the applicability of Murray's law to xylem. A challenge for the future is to develop a better understanding of the interaction between tree biomechanics, hydraulics and growth. □

## Methods

A computer programme calculated the hydraulic conductance per fixed vascular volume of a branched transport network. We modelled a constant-volume vascular network with specified number of ranks, a branch furcation number,  $B$  ( $B = 2$ , dichotomous,  $B = 3$ , trichotomous, and so on), and  $F$ . We standardized  $F$  to equal 1 for the pipe model and 2 for the aorta model regardless of  $B$  ( $F = [(F' - 1)/(B - 1)] + 1$ , where  $F'$  is the raw conduit furcation number). The network had constant  $F$  across ranks, and constant fractional taper in conduit diameter across ranks (diameter was constant within rank). The number of conduits at the distal rank was one per branch—the minimum required to vascularize the system. Rank length was unity, because the Murray's law solution is independent of branch length. To generate Fig. 2a, we varied conduit taper and computed the network conductance. To generate Fig. 2b, conduit taper was set to match Murray's law, and network hydraulic conductance computed as  $F$  was changed.

Conduit measurements were made on species with compound leaves (Table 1) collected in the greater Salt Lake City (Utah) area (40° 46' N, 111° 58' W). Three to four individuals per species were collected from the same habitat, and were similar in size. Upon collection, plants were perfused with 0.05% basic fuchsin to determine which xylem conduits were functional, and only these were measured. Between 2,000 and 6,000 conduits were measured per individual. Conduit radii were measured at the petiole and petiole rank for leaves, and at the current year's annual bud scar in stems (Table 1).

Conduit statistics per rank had to be estimated, given the large numbers of conduits involved. In leaves, all conduits in petioles and petioles were measured in a sample of  $\geq 5$  leaves. Each measured leaf provided a  $\Sigma r^x$  per leaf area which was multiplied by total leaf area to estimate rank  $\Sigma r^x$ . In secondary stem xylem, conduits in  $\geq 3$  radial sectors per branch were measured, with each sector yielding a  $\Sigma r^x$  per sector area. Each subsample was multiplied by total xylem area of the rank to obtain a rank  $\Sigma r^x$  estimate. These multiple  $\Sigma r^x$  estimates per rank were incorporated into the analysis of variance (ANOVA).

To test Murray's law, the  $\Sigma r^x$  of the distal-most rank (petiole) was compared against the  $\Sigma r^x$  of each proximal rank (petiole, stem xylem at first year bud scar). To test the conservation of  $\Sigma r^3$ ,  $x$  in each of the rank estimates of  $\Sigma r^x$  was incremented from 1 to 5. Raising the  $\Sigma r^x$  to relatively high  $x$  resulted in frequency distributions that were not normally distributed, so the data were log-transformed for statistical analyses. For each species we used a 2-way ANOVA with the  $\Sigma r^x$  estimates as the dependent variable, the distal-most versus proximal rank pair as the fixed factor, and the replicate individuals as a random factor (for the petiole: petiole comparison there were 26 degrees of freedom for PQ, CR and FP; and 45 for AN (see Table 1 for nomenclature); for the petiole:1-yr-old wood comparison, there were 25 degrees of freedom for PQ, 21 for CR and 43 for FP<sup>27</sup> (SPSS Version 8.0.0 (SPSS, Chicago, 1998)). Increased similarity in estimates of  $\Sigma r^x$  between ranks resulted in  $P$ -values approaching 1. For each paired comparison we used a 2-way ANOVA to identify the range of  $x$  over which  $\Sigma r^x$  between ranks was not significantly different at  $P \geq 0.05$ . If this range of  $x$  did not include 3, Murray's law was rejected for that comparison.

Received 9 September 2002; accepted 21 January 2003; doi:10.1038/nature01444.

- Hubbard, R. M., Stiller, V., Ryan, M. G. & Sperry, J. S. Stomatal conductance and photosynthesis vary linearly with plant hydraulic conductance in ponderosa pine. *Plant Cell Environ.* **24**, 113–121 (2001).
- Saliendra, N. Z., Sperry, J. S. & Comstock, J. P. Influence of leaf water status on stomatal response to humidity, hydraulic conductance, and soil drought in *Betula occidentalis*. *Planta* **196**, 357–366 (1995).
- Meinzer, F. C. *et al.* Environmental and physiological regulation of transpiration in tropical forest gap species: The influence of boundary layer and hydraulic properties. *Oecologia* **101**, 514–522 (1995).
- Sperry, J. S., Alder, N. N. & Eastlack, S. E. The effect of reduced hydraulic conductance on stomatal conductance and xylem cavitation. *J. Exp. Bot.* **44**, 1075–1082 (1993).
- Meinzer, F. C. & Grantz, D. A. Stomatal and hydraulic conductance in growing sugarcane: Stomatal adjustment to water transport capacity. *Plant Cell Environ.* **13**, 383–388 (1990).
- West, G. B., Brown, J. H. & Enquist, B. J. A general model for the origin of allometric scaling laws in biology. *Science* **276**, 122–126 (1997).
- West, G. B., Brown, J. H. & Enquist, B. J. A general model for the structure and allometry of plant vascular systems. *Nature* **400**, 664–667 (1999).
- Enquist, B. J., West, G. B. & Brown, J. H. in *Scaling in Biology* (eds Brown, J. H. & West, G. B.) 167–198 (Oxford Univ. Press, Oxford, 2000).
- Richter, J. P. *The Notebooks of Leonardo da Vinci (1452–1519), Compiled and Edited from the Original Manuscripts* (Dover, New York, 1970).
- Horn, H. S. in *Scaling in Biology* (eds Brown, J. H. & West, G. B.) 199–220 (Oxford Univ. Press, Oxford, 2000).
- Murray, C. D. The physiological principle of minimum work. I. The vascular system and the cost of blood volume. *Proc. Natl Acad. Sci. USA* **12**, 207–214 (1926).
- Horn, H. S. *The Adaptive Geometry of Trees* (Princeton Univ. Press, Princeton, New Jersey, 1971).
- Givnish, T. J. in *On the Economy of Plant Form and F* (ed. Givnish, T. J.) 3–9 (Cambridge Univ. Press, Cambridge, 1986).
- Gould, S. J. & Lewontin, R. C. The spandrels of San Marco and the Panglossian paradigm: a critique of the adaptationist programme. *Proc. R. Soc. Lond. B* **205**, 581–598 (1979).
- Mark, R. Architecture and evolution. *Am. Sci.* **84**, 383–389 (1996).

- Raven, J. A. The evolution of vascular land plants in relation to supracellular transport processes. *Adv. Bot. Res.* **5**, 153–219 (1987).
- Sherman, T. F. On connecting large vessels to small: The meaning of Murray's law. *J. Gen. Physiol.* **78**, 431–453 (1981).
- LaBarbera, M. Principles of design of fluid transport systems in zoology. *Science* **249**, 992–999 (1990).
- Vogel, S. *Life in Moving Fluids: The Physical Biology of Flow* (Princeton Univ. Press, Princeton, New Jersey, 1994).
- Canny, M. J. The transpiration stream in the leaf apoplast: Water and solutes. *Phil. Trans. R. Soc. Lond. B* **341**, 87–100 (1993).
- Hacke, U. G., Sperry, J. S., Pockman, W. P., Davis, S. D. & McCulloh, K. A. Trends in wood density and structure are linked to prevention of xylem implosion by negative pressure. *Oecologia* **126**, 457–461 (2001).
- Shinozaki, K., Yoda, K., Hozumi, K. & Kira, T. A quantitative analysis of plant form—the pipe model theory: I. Basic analysis. *Jpn. J. Ecol.* **14**, 97–105 (1964).
- Sokal, R. R. & Rohlf, F. J. *Biometry: The Principles and Practice of Statistics in Biological Research* (Freeman, New York, 1995).
- Zimmermann, M. H. in *Xylem Structure and the Ascent of Sap* (ed. Timell, T. E.) 15–16, 99 (Springer, Berlin, 1983).
- Keller, J. B. & Niordson, F. I. The tallest column. *J. Math. Mech.* **16**, 433–446 (1966).
- McMahon, T. A. Size and shape in biology. *Science* **179**, 1201–1204 (1973).
- Grafen, A. & Hails, R. *Modern Statistics for the Life Sciences* (Oxford Univ. Press, Oxford, 2002).

Supplementary Information accompanies the paper on Nature's website (<http://www.nature.com/nature>).

**Acknowledgements** We thank A. Collopy and M. McCord for assistance in collecting plants. This work was partly supported by Sigma Xi (K.A.M.) and NSF (J.S.S.).

**Competing interests statement** The authors declare that they have no competing financial interests.

**Correspondence** and requests for materials should be addressed to K.A.M. (e-mail: mcculloh@biology.utah.edu).

## Extra-embryonic function of Rb is essential for embryonic development and viability

Lizhao Wu\*, Alain de Bruin\*, Harold I. Saavedra\*, Maja Starovic†, Anthony Trimboli\*, Ying Yang‡, Jana Opavska\*, Pamela Wilson§, John C. Thompson§, Michael C. Ostrowski§||, Thomas J. Rosol||¶, Laura A. Woollett#, Michael Weinstein§||, James C. Cross†, Michael L. Robinson‡||☆ & Gustavo Leone\*§||

\* Human Cancer Genetics Program, Department of Molecular Virology, Immunology and Medical Genetics, § Department of Molecular Genetics, || Comprehensive Cancer Center, ¶ Department of Veterinary Biosciences, and ☆ Department of Pediatrics, The Ohio State University, Columbus, Ohio 43210, USA

† Department of Biochemistry & Molecular Biology, University of Calgary Faculty of Medicine, Calgary, Alberta T2N 4N1, Canada

‡ Division of Molecular and Human Genetics, Children's Research Institute, Columbus, Ohio 43205, USA

# Department of Pathology and Laboratory Medicine, University of Cincinnati Medical Center, Cincinnati, Ohio 45267, USA

The retinoblastoma (*Rb*) gene was the first tumour suppressor identified<sup>1</sup>. Inactivation of *Rb* in mice results in unscheduled cell proliferation, apoptosis and widespread developmental defects, leading to embryonic death by day 14.5 (refs 2–4). However, the actual cause of the embryonic lethality has not been fully investigated. Here we show that loss of *Rb* leads to excessive proliferation of trophoblast cells and a severe disruption of the normal labyrinth architecture in the placenta. This is accompanied by a decrease in vascularization and a reduction in placental transport function. We used two complementary techniques—tetraploid aggregation and conditional knockout strategies—to demonstrate that *Rb*-deficient embryos supplied